Dimeric N-Terminal Segment of Human Surfactant Protein B (dSP-B_{1-25}) Has Enhanced Surface Properties Compared to Monomeric SP-B_{1-25}

Edwin J. A. Veldhuizen,* Alan J. Waring,† Frans J. Walther,† Joseph J. Batenburg,* Lambert M. G. van Golde,* and Henk P. Haagsman*‡

*Department of Biochemistry and Cell Biology, Faculty of Veterinary Medicine, Utrecht University, 3508 TD Utrecht, the Netherlands; †Department of Pediatrics, Charles Drew University, Los Angeles, California 90059, and Perinatal Research Laboratories, Harbor-UCLA Research and Education Institute, Torrance, California 90502 USA; and ‡Department of Science of Food of Animal Origin, Utrecht University, 3508 TD, Utrecht, the Netherlands

ABSTRACT Surfactant protein B (SP-B) is a 17-kDa dimeric protein produced by alveolar type II cells. Its main function is to lower the surface tension by inserting lipids into the air/liquid interface of the lung. SP-B's function can be mimicked by a 25-amino acid peptide, SP-B_{1-25}, which is based on the N-terminal sequence of SP-B. We synthesized a dimeric version of this peptide, dSP-B_{1-25}, and the two peptides were tested for their surface activity. Both SP-B_{1-25} and dSP-B_{1-25} showed good lipid mixing and adsorption activities. The dimeric peptide showed activity comparable to that of native SP-B in the pressure-driven captive bubble surfactometer. Spread surface films led to stable near-zero minimum surface tensions during cycling while protein free, and films containing SP-B_{1-25} lost material from the interface during compression. We propose that dimerization of the peptide is required to create a lipid reservoir attached to the monolayer from which new material can enter the surface film upon expansion of the air/liquid interface. The dimeric state of SP-B can fulfill the same function in vivo.

INTRODUCTION

Pulmonary surfactant is a mixture of lipids and specific proteins that is secreted into the alveolar fluid by alveolar type II cells. Its main function is to reduce the surface tension at the air/liquid interface in the lung. This is achieved by forming a surface film that consists of a monolayer that is highly enriched in dipalmitoylphosphatidylcholine (DPPC) and bilayer lipid/protein structures closely attached to it. This surface film reduces the work of breathing and prevents alveolar collapse upon end expiration. The in vivo existence of such a film has recently been confirmed by electron microscopy (Schürch et al., 1995).

The highly hydrophobic surfactant-specific proteins B and C (SP-B and SP-C) are required for a rapid insertion of new material from the lipid bilayer structures to the monolayer upon inspiration. In addition to reducing the work required for breathing, this prevents serum components from entering the surface film. These serum components, of which albumin is the most abundant, disturb surfactant function, and an increase in these serum components in the bronchoalveolar lavage is often observed in several diseases related to surfactant dysfunction (Byrne et al., 1992; Hallman et al., 1989; Jorens et al., 1992; Matsumoto et al., 1992; Nakos et al., 1997). SP-B and SP-C are also likely involved in the DPPC enrichment of the monolayer (for a review see Pérez-Gil and Keough, 1998). A monolayer enrichment of DPPC is required to create stable surface films with near-zero surface tensions.

SP-B is a ~17 kDa homodimer. Secondary structure analysis and homology with related proteins, especially members of the saposin-like family (Patthy, 1991), predict an SP-B structure that contains four amphipathic α-helices (Andersson et al., 1995). These helices are thought to interact with the surfactant lipids, with a specific interaction between anionic lipids and the positive charges of SP-B (Baatz et al., 1990; Longo et al., 1993). The structure of SP-C, a 4.2-kDa protein containing 35 amino acids, has been completely resolved in solution and micelles by NMR (Johansson et al., 1994). Its main characteristics are a polyvalyl α-helix that can exactly span a lipid bilayer and a tail that contains two palmitoylated cysteines.

The importance of SP-B in surfactant is apparent from the lethal respiratory distress that is caused by SP-B deficiency in humans (Nogee et al., 1994) and in SP-B knock-out mice (Tokieda et al., 1997). A lowered or total lack of all surfactant components, due to immaturity of the lungs in premature infants or inflammation or trauma in adults, leads to respiratory distress syndrome (RDS). Administration of exogenous surfactant has been proven a successful strategy for treating the neonatal form of RDS, and improvements are observed in ARDS as well (for a review see Robertson and Halliday, 1998). However, human surfactant is scarce, and therefore replacement surfactants are derived from animals. The disadvantage of this is that immunological responses and viral infections of the treated patient might occur. A completely synthetic surfactant might overcome these problems, and a major research area has evolved in this direction.

The development of a purely synthetic surfactant requires a thorough understanding of the role of the protein and lipid components in pulmonary surfactant. Several peptides

Received for publication 22 November 1999 and in final form 14 March 2000.

Address reprint requests to Dr. Henk P. Haagsman, Department of Biochemistry and Cell Biology, Faculty of Veterinary Medicine, Utrecht University, P.O. Box 80.176, 3508 TD Utrecht, the Netherlands. Tel.: +31-30-2535354; Fax: +31-30-2535492; E-mail: H.P.Haagsman@vvdo.vet.uu.nl.

0006-3495/00/07/377/08 $2.00

based on either SP-B or SP-C have been tested (Bruni et al., 1991, 1998; Johansson et al., 1995; Nilsson et al., 1998; Takei et al., 1996). SP-$B_{1–25}$ is a peptide based on the N-terminal segment of human SP-B (hSP-B) and has been shown to have an amphipathic helical structure (Gordon et al., 1996). It has a high affinity for phospholipid monolayers and increases the collapse pressure of palmitic acid (PA) monolayers (Lipp et al., 1996; Waring et al., 1989). The peptide also permits resistance to the inhibitory effect of plasma constituents that inhibit surfactant and partly restores lung compliance in two animal models (Bruni et al., 1998). All of these activities are known characteristics of native SP-B. To mimic the dimeric state of native SP-B we synthesized the new peptide dSP-$B_{1–25}$. The monomers of this dimer differ from the previously mentioned SP-$B_{1–25}$ in that a cysteine at position 11 was substituted by alanine, leaving only one cysteine in the peptide. A disulfide linkage between two cysteines of the monomers results in a dimer of the SP-$B_{1–25}$ peptide (Fig. 1). The activity of both peptides was tested in vitro, using the captive bubble surfactometer (CBS) and lipid mixing experiments. Both peptides show good activity in several aspects of surface film formation and dynamics, with a clear positive effect of the dimerization on the respreadability of lipids under dynamic conditions.

EXPERIMENTAL PROCEDURES

Materials

1,2-Dipalmitoyl-*sn*-glycero-3-phosphocholine (DPPC) and 1-palmitoyl-2-oleoyl-*sn*-glycero-3-phospho-*rac*-(1-glycerol) (POPG) were obtained from Avanti Polar Lipids (Alabaster, AL); 1-palmitoyl-2-(1-pyrenedecanoyl)-*sn*-glycero-3-phosphocholine (pyrene-PC) was from Molecular Probes; HEPES was from Life Technologies (Paisley, Scotland); EDTA, calcium chloride ($CaCl_2$), chloroform ($CHCl_3$), and methanol (MeOH) were from Baker Chemicals B.V. (Deventer, the Netherlands). Organic solvents were distilled before use. hSP-B and hSP-C were isolated from amniotic fluid, using protocols normally used for lung lavage, as described previously (Oosterlaken Dijksterhuis et al., 1991).

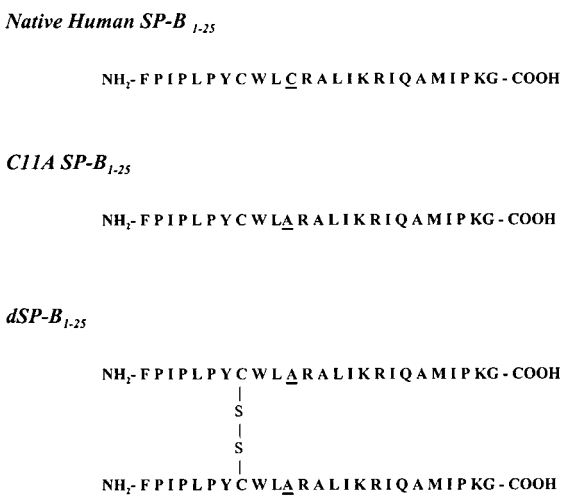

FIGURE 1 The sequence of SP-$B_{1–25}$ and dSP-$B_{1–25}$ in one-letter code.

Peptide synthesis

Molecular design rational

Using the known residue-specific secondary structure of SP-$B_{1–25}$ (Gordon et al., 2000) (Fig. 2), we made modifications in the amino acid sequence to make it more closely emulate the structure and function of the native protein. Cys^{11} was replaced with Ala to provide a single disulfide link at the N-terminal helical residue Cys^{8}, allowing the formation of a unique C11A SP-$B_{1–25}$ homodimer. This dimeric peptide will be referred to as dSP-$B_{1–25}$.

Solid-phase peptide synthesis, purification, and characterization of SP-$B_{1–25}$ and dSP-$B_{1–25}$

The SP-$B_{1–25}$ peptide and dSP-$B_{1–25}$ monomer (C11A SP-$B_{1–25}$) were synthesized on a 0.25-mmol scale with an Applied Biosystems model 431A peptide synthesizer, using a FastMoc strategy (Fields et al., 1991). The peptides were synthesized with prederivatized Fmoc-Gly resin (Calbiochem-Nova, La Jolla, CA) or PEG-PA resin (Perceptive Biosystems, Old Connecticut Path, MA) and were single-coupled for all residues.

Crude peptide product was purified by reverse-phase high performance liquid chromatography with a Vydac reverse-phase C8-column (Vydac, Hesperia, CA), using a linear gradient of water:acetonitrile (0–100% acetonitrile with 0.1% trifluoroacetate as an anion pairing agent) over a period of 1 h. Purified peptide was freeze-dried twice at a concentration of 5 mg peptide/ml from acetonitrile:10 mM HCl solutions to remove acetate counterions that interfere with dimerization and in vivo or in vitro measurements. The molecular mass of the monomeric SP-$B_{1–25}$ peptides was confirmed by fast atom bombardment mass spectroscopy or electrospray mass spectroscopy. Masses of 2926.7 and 2895.5 Da were observed for SP-$B_{1–25}$ and C11A SP-$B_{1–25}$, respectively, which correlates well with the calculated masses.

For the formation of the dimer peptide, C11A SP-$B_{1–25}$ monomer was first reduced with 100 mM dithiothreitol (DTT) in trifluoroethanol (TFE):10 mM sodium phosphate buffer pH 7.5 (1:1, v/v) at a concentration of 1 mg peptide/ml solution for 12 h before oxidation. The peptide solution was then passed through a Sephadex P-10 size exclusion column using TFE:10 mM sodium phosphate buffer (pH 7.5) (1:1, v/v) to remove the reducing agent before oxidation-disulfide formation. The isolated peptide solution was then freeze-dried overnight to remove solvent. The dry peptide powder was dissolved in TFE:10 mM sodium phosphate buffer (pH 7.5) (1:1, v/v) at a concentration of 1–2 mg peptide/ml and stirred vigorously for 24 h to facilitate the air-mediated oxidation of the peptide monomers to form a disulfide-linked homodimer dSP-$B_{1–25}$ (preferred method of dimer formation). The molecular mass of the peptide was confirmed by electrospray mass spectroscopy and indicated the yield of dimeric product to be essentially 100%. The mass spectrum shows five

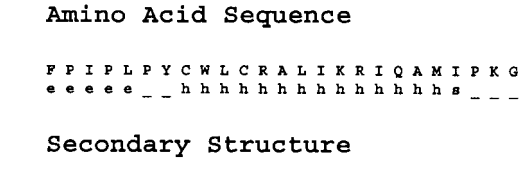

FIGURE 2 The amino acid sequence and specific secondary structure of SP-$B_{1–25}$ in surfactant lipid (Gordon et al., 2000; Protein Data Bank ID: 1DFW). Residue specific secondary assignments are as follows: h, helix; e, extended; s, bend; _, disordered.

major peaks with masses of 579.8, 725.0, 828.1, 966.2, and 1159.4 Da, which all arise from the peptide (the 10, 8, 7, 6, and 5^+ ions, respectively) with an observed average mass of 5790.8 Da. This is very close to the calculated mass of 5791.2 Da. The concentrations of peptides and native surfactant proteins for control experiments were determined by quantitative amino acid analysis (UCLA Microsequencing Facility, Los Angeles, CA, and Eurosequence bv, Groningen, the Netherlands).

Vesicle preparation

Small unilamellar vesicles (SUVs) for lipid mixing and captive bubble surfactometer experiments were prepared as follows. Lipids from stock solutions in $CHCl_3$/MeOH with or without peptides in $CHCl_3$/MeOH were dried under a continuous stream of nitrogen at room temperature. The resulting lipid/peptide film was rehydrated by adding the appropriate buffer, vortexing, and incubating at 55°C for 15 min. The multilamellar vesicles thus formed were sonicated for 2 × 1 min at 55°C with a 10-s interval. The vesicles were cooled to 37°C and used immediately.

Lipid mixing

Lipid mixing experiments were performed as described by Oosterlaken-Dijksterhuis (Oosterlaken-Dijksterhuis et al., 1992). Phospholipid SUVs (300 nmol of lipid) with or without peptides were mixed with pyrene-PC-labeled SUVs (15 nmol of lipid containing 10% pyrene-PC) in a HEPES buffer (25 mM, pH 7.0) supplemented with 0.2 mM EGTA at a final volume of 2 ml. A standard concentration of 0.4 mol% was used for the two peptides and hSP-B, and an additional experiment with a twofold concentration for SP-B_{1-25} was performed. Fluorescence emission spectra were recorded before and after the addition of 30 μl 0.3M $CaCl_2$ on a Perkin-Elmer LS 50 fluorescence spectrophotometer. The excitation wavelength was 343 nm, and the emission between 360 and 550 nm was recorded. The excimer/monomer (E/M) ratio, indicative of the amount of lipid mixing, was calculated by dividing the intensity at 475 nm (excimer fluorescence) by the intensity at 377 nm (monomer fluorescence).

Captive bubble surfactometry

The activity of the synthetic SP-B analogs in inserting lipids into the air/liquid interface was determined using a pressure-driven captive bubble surfactometer (Putz et al., 1994). A bubble (0.5 cm^2) was formed in subphase buffer (140 mM NaCl, 10 mM HEPES, 0.5 mM EDTA, 2.5 mM $CaCl_2$, pH 6.9) by injecting air (28.5 μl) into the sample chamber at 1.0 bar and 37°C. Two methods of surface film formation were used, i.e., film spreading and adsorption from the subphase.

Film spreading

Stock solutions of DPPC:POPG with a molar composition of 8:2 with or without proteins were prepared in $CHCl_3$:MeOH (1:1, v/v). From this stock solution 0.05 μl (0.25 nmol lipids) was spread at the air/water interface with a glass syringe. The subphase was stirred for 60 min to enhance the desorption of solvent, after which the sample chamber was perfused for 30 min with 7 ml buffer. Subsequently, 50 μl SUV (DPPC:POPG, 80:20 mol/mol) was injected into the subphase (final concentration 200 μg PL/ml), and stirring was continued for another 15 min. The bubble area was increased by sudden lowering of the pressure to 0.5 bar for 10 s. Subsequently, the bubble was cycled five times between two preset pressure values of 0.5 and 2.8 bar in 1 min, resulting in a dynamic compression and expansion of the air bubble. After the cycling procedure, another 15-min adsorption time was allowed, followed by a second series of five cycles. A video camera continuously monitored the shape of the bubble, from which the surface tension values were calculated (Putz et al., 1998).

Film adsorption

SUVs of DPPC: POPG (8:2, mol/mol) or DPPC:POPG:PA (7:2:1) with or without proteins were prepared as described and injected directly into the sample chamber. The final concentration in the subphase was 200 μg lipids/ml. The material was allowed to adsorb to the interface of the bubble for 15 min, followed by the same cycling and readsorption period described above. The extra adsorption period between the cycle series was introduced after pilot experiments with the peptides. These revealed that new material could be adsorbed from the subphase to the monolayer after the first cycling series to give rise to lower starting surface tensions at 1 bar for the second series and lower surface tensions during cycling.

RESULTS

Lipid mixing

The peptides SP-B_{1-25} and dSP-B_{1-25} were tested for their activity to induce lipid mixing. When donor vesicles containing pyrene-PC are mixed with acceptor vesicles (initiated by the addition of calcium ions), the fluorescent lipid probe becomes diluted, leading to more monomeric fluorescence and less excimeric fluorescence. The results are depicted in Fig. 3; they show that both SP-B-based peptides have an activity comparable to that of hSP-B. SP-B_{1-25} has a slightly lower activity based on molar concentrations, but doubling the amount of SP-B_{1-25} (to achieve the same amount of protein by weight compared to dSP-B_{1-25}) diminishes this difference.

Captive bubble surfactometry

Adsorption

With the captive bubble surfactometer, several aspects of surface film formation and dynamics can be investigated. The adsorption of material from vesicles in the subphase to

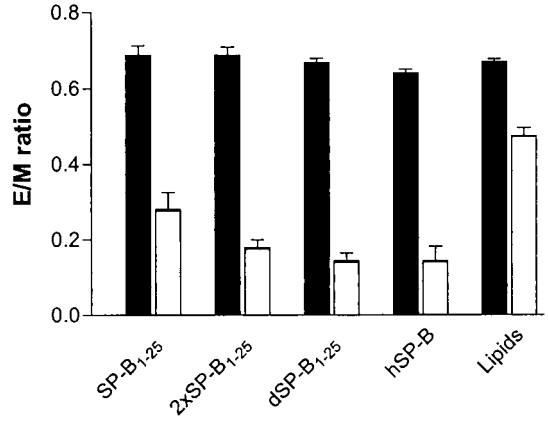

FIGURE 3 Effect of SP-B analogs on lipid mixing. Black bars represent the E/M ratio before and white bars the E/M ratio after calcium addition. 2× SP-B_{1-25} has a twofold increased peptide concentration (0.8%) compared to dSP-B_{1-25} and hSP-B. Values shown are the average of at least four separate experiments ± SEM.

a clean interface of the air bubble in the cuvette is easily detected by a change in the shape of the bubble during the adsorption period. Lipid SUVs containing the synthetic peptides or control vesicles were injected into the cuvette and allowed to adsorb for 15 min. No significant change in surface tension was detected after this time period. The final surface tensions are depicted in Table 1. Using DPPC:POPG (8:2, mol/mol) vesicles, we found that the SP-B analogs show a clear activity compared to protein-free samples (40 and 43 mN/m versus 53 mN/m for the protein-free sample). However, the values are significantly higher than the values for hSP-B or hSP-C (23 and 28 mN/m). Increasing the protein concentration to 3 mol% did not induce an increased adsorption, showing that the amount of protein is not the limiting factor in this process. Using DPPC:POPG:PA (7:2:1) vesicles also did not affect the adsorption kinetics of either of the synthetic analogs or of hSP-B, although slightly lower surface tension values and a tendency toward concentration dependence were observed for SP-$B_{1–25}$.

Cycling of adsorbed films

DPPC:POPG vesicles

The maximum and minimum surface tensions (γ_{max} and γ_{min}) during cycling with the DPPC:POPG mixture are shown in Fig. 4. Both SP-$B_{1–25}$ and dSP-$B_{1–25}$ show increased activity compared to protein-free samples, with a 10^{th}-cycle γ_{max} value of 57 mN/m for SP-$B_{1–25}$ and 48 mN/m for dSP-$B_{1–25}$ (versus 60 mN/m for protein-free vesicles), while the γ_{min} values are ~12 mN/m (versus 20 mN/m for the protein-free sample). However, the peptides are significantly less active than hSP-B or hSP-C (not shown). These proteins reach near-zero surface tensions upon the first (hSP-B) or the sixth cycle (hSP-C, the first cycle after the extra adsorption period). The maximum values are also significantly lower for the native proteins than those for the peptides. Increasing the peptide concentration to 3 mol% gave rise to some improvement for both SP-$B_{1–25}$ and dSP-$B_{1–25}$, but they were still not comparable to the native protein (results not shown). Interestingly, the dimer peptide always shows better activity than the monomer peptide. Even when 3% SP-$B_{1–25}$ is compared to 1% dSP-$B_{1–25}$ (which also means on a weight basis more monomer peptide), the dimer has significantly lower γ_{max} values.

TABLE 1 Surface tensions (in mN/m) after 15-min adsorption of peptide-containing vesicles

Mol% peptide	DPPC:POPG vesicles	DPPC:POPG:PA vesicles
None	53.2 ± 2.6	53.1 ± 3.9
3% hSP-C	27.9 ± 2.5	Not done
1% hSP-B	22.6 ± 0.34	24.9 ± 2.0
1% SP-$B_{1–25}$	40.6 ± 1.5	42.8 ± 1.6
2% SP-$B_{1–25}$	41.1 ± 1.0	40.6 ± 1.8
3% SP-$B_{1–25}$	42.5 ± 0.9	37.1 ± 2.3
1% dSP-$B_{1–25}$	36.3 ± 0.4	40.2 ± 0.9
3% dSP-$B_{1–25}$	38.3 ± 1.4	Not done

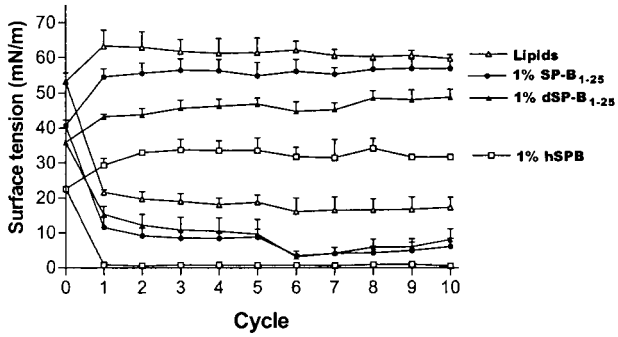

FIGURE 4 Maximum and minimum surface tensions during cycling of adsorbed films from DPPC:POPG (8:2) SUV. Two hundred micrograms of SUVs was injected into the subphase and allowed to adsorb to the interface for 15 min. Then cycling was performed by varying the pressure between 0.5 and 2.8 bar. The values shown are the average of at least three separate experiments ± SEM.

DPPC:POPG:PA vesicles

The addition of PA to the lipid mixture gave rise to dramatic effects, especially on the minimum surface tensions (Fig. 5 *A*). One percent dSP-$B_{1–25}$ reached near-zero γ_{min} values upon the first cycle, comparable to hSP-B (result not shown), while the γ_{max} value (42.5 mN/m for the 10th cycle) is also significantly lower compared to the PA-free experiments. The same effect is observed for the monomer, but only at higher concentrations (Fig. 5 *B*). The 2% SP-$B_{1–25}$ sample reached near-zero γ_{min} values with the sixth cycle, while 3% SP-$B_{1–25}$ was completely comparable to 1% dSP-$B_{1–25}$. In contrast to the peptide samples, no effect of PA was observed when hSP-B was used. Furthermore, when as little as 0.02% SP-B (which is below the optimum SP-B concentration) was incorporated into the SUVs, equal γ_{max} and γ_{min} values were detected with or without PA (results not shown).

Spread films

The advantage of spread films over adsorbed films is that, at the start of the experiment, the exact composition of the surface film is known. Lipids (0.25 nmol) with or without peptide were spread at the air/liquid interface, and cycling was performed as described in the experimental procedures. Fig. 6 shows that SP-$B_{1–25}$ at a concentration of 2% reaches a near-zero surface tension upon the first cycle, which then steadily increases with each cycle. This is interpreted as irreversible loss of material during compression of the bubble (especially when the bubble is compressed beyond the point where minimal surface tension is reached—overcom-

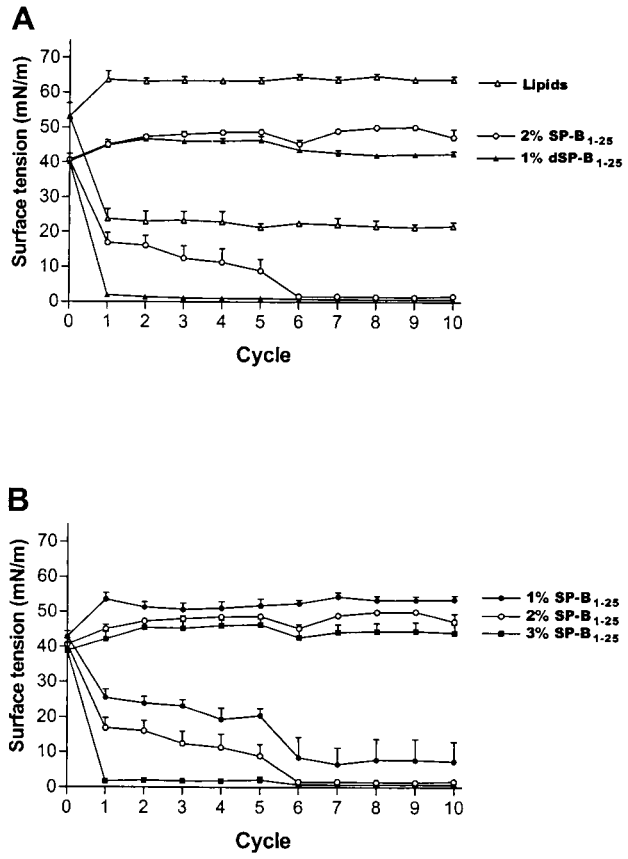

FIGURE 5 Maximum and minimum surface tensions during cycling of adsorbed films from DPPC:POPG:PA (7:2:1) SUV. Two hundred micrograms of SUVs was injected into the subphase and allowed to adsorb to the interface for 15 min. Then cycling was performed by varying the pressure between 0.5 and 2.8 bar. The values shown are the average of at least three separate experiments ± SEM.

pression). A similar behavior for the protein-free lipid sample is seen, in contrast to a stable γ_{min} value throughout the whole cycling procedure for 1% dSP-B_{1-25} and native SP-B.

The γ_{max} values of the dSP-B_{1-25} sample are also significantly lower than that of 1% (results not shown) or 2% SP-B_{1-25} and reach values close to native SP-B values (59, 46, and 40 mN/m for SP-B_{1-25}, dSP-B_{1-25}, and hSP-B, respectively). The increasing γ_{max} values upon cycling for SP-B_{1-25} are not observed after the second cycle for native SP-B and dSP-B_{1-25}.

Refinement of the surface film

Surface tension-area isotherms show valuable information on refinement of the monolayer upon cycling. A representative curve is shown in Fig. 7 *A* for 1% dSP-B_{1-25} (using adsorbed films from DPPC:POPG:PA vesicles) and 0.02% hSP-B (Fig. 7 *B*). This figure shows that the dSP-B_{1-25} film

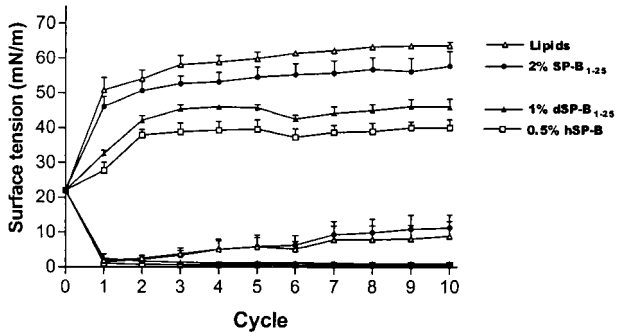

FIGURE 6 Maximum and minimum surface tensions during cycling of spread films of DPPC:POPG (8:2). Peptide/lipid mixtures were dissolved in $CHCl_3$/MeOH. Lipids (0.25 nmol) in 0.05 μl were spread at the interface. The subphase was washed, and vesicles without peptides were injected into the subphase. Then cycling was performed by varying the pressure between 0.5 and 2.8 bar. The values shown are the average of at least three separate experiments ± SEM.

requires less area reduction on consecutive cycles to reach low surface tensions and that dSP-B_{1-25} surface films require larger reductions to reach these low tensions than hSP-B films. However, because each cycle starts from a

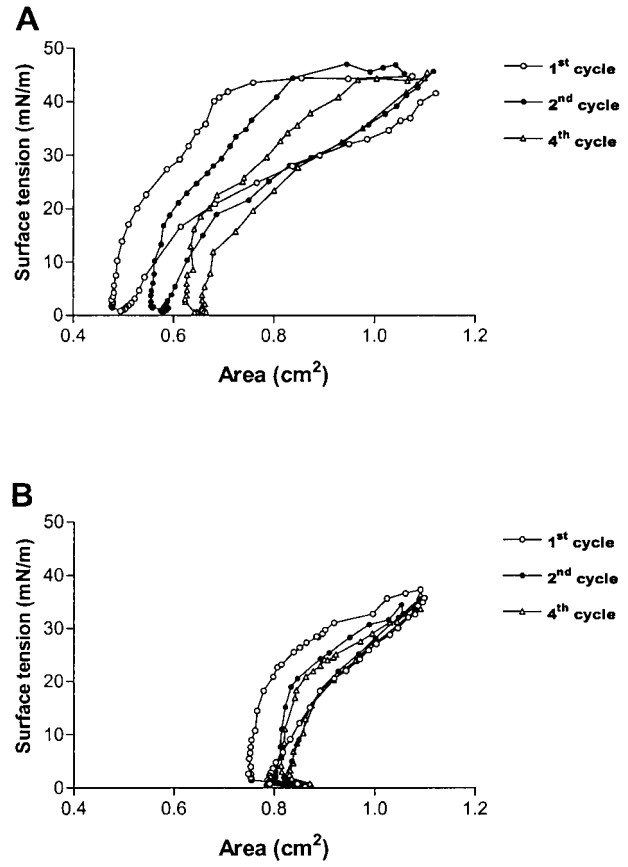

FIGURE 7 Representative surface tension-area isotherms of adsorbed films of 1% dSP-B_{1-25} (*A*) and 0.02% hSP-B (*B*).

different γ_{max} (with significantly lower values for hSP-B), they cannot be compared directly. Therefore, the area reductions needed to reach surface tensions of <2 mN/m from 20 mN/m were calculated. For the dSP-$B_{1–25}$ samples these reductions fell from 34.3 ± 1.5% in the first cycle to 26.4 ± 0.6% and 19.1 ± 2.7% in the second and fourth cycles, respectively. This indicates that the monolayer is enriched in DPPC during the cycling procedure. The isotherms of SP-$B_{1–25}$ were comparable (when 3% SP-$B_{1–25}$ was used) to the one shown for dSP-$B_{1–25}$. The calculated area reductions needed for the decrease from 20 to 2 mN/m were 37.2 ± 4.5%, 26 ± 3.5%, and 25 ± 3.1% for the first, second, and fourth cycles. Fig. 7 *B* shows a typical surface tension-area isotherm of 0.02% hSP-B. The decrease in area reduction required to reach 2 mN/m upon cycling is almost absent in this experiment. The calculated values are 24 ± 3.6%, 19 ± 4.3%, and 19 ± 5.6% for the first, second, and fourth cycles, respectively.

DISCUSSION

In this paper the in vitro surface activity of two synthetic SP-B analogs, based on the N-terminal segment of human SP-B, was tested. The monomeric SP-$B_{1–25}$ shows a clear activity compared to nonprotein samples. dSP-$B_{1–25}$, the dimeric peptide, shows an even better activity in some aspects of surface film dynamics, especially respreadability of lipids, which resembles the native protein activity.

The lipid mixing activities of dSP-$B_{1–25}$ and SP-$B_{1–25}$ were found to be similar to native SP-B (Fig. 3). The fusogenic properties are thought to be important in surfactant function in several aspects. They likely play a role in forming contact points between the lipid monolayer at the air/liquid interface and the bilayer structures that are attached to it. This enables the lung to insert new material into the interface when the surface is enlarged (during inspiration) to maintain a relatively low surface tension. Fusogenic events are also thought to be important in the formation of tubular myelin, which contains highly curved structures at the edges of the tubules where lipid bilayers merge.

The adsorption of lipids to a clean air/liquid interface from vesicles in the subphase was clearly stimulated by the presence of SP-$B_{1–25}$ or dSP-$B_{1–25}$. However, the values obtained were, in all of the experiments performed, ~15 mN/m or more above the observed equilibrium surface tension of 23 mN/m (Table 1). This indicates that the peptides cannot penetrate an existing, relatively tightly packed monolayer with a surface tension of 35 mN/m and fuse with it. These results are in line with results that were obtained for SP-$B_{1–25}$ with a Langmuir-Wilhelmy balance (Bruni et al., 1991). In those experiments it was observed that if lipid films were spread to an initial surface pressure of ~42 mN/m (surface tension of 30 mN/m), no insertion of peptide could occur. However, in our experiments it was observed that "extra" adsorption can occur despite the existing monolayer after the first cycling series. Somehow, because of the cycling procedure, new material from peptide-containing vesicles was now capable of inserting into the interface. A possible explanation for this phenomenon is that cycling has induced a lipid reservoir, probably consisting of lipid bilayer structures in close contact with the monolayer at the interface. The contact points between the monolayer and the reservoir would then allow an easy adsorption of new lipids into the interface, despite the relatively low surface tension of ~40 mN/m, which prevents adsorption from "normal" subphase vesicles.

The cycling experiments with spread films show that dSP-$B_{1–25}$ films but not SP-$B_{1–25}$ give rise to stable, near-zero γ_{min} during the whole cycling procedure. This shows that the material that is squeezed out during compression stays attached to the monolayer and is directly available for reinsertion upon the next expansion. Insertion of new lipids from the subphase vesicles occurs at a much slower rate and will therefore only play a minor role during the dynamic cycling. The easiest explanation for the observed difference is that dSP-$B_{1–25}$ can form a bridge between the monolayer and the squeezed-out subphase lipids by attaching one monomer part to each membrane structure. SP-$B_{1–25}$ does not offer this possibility, and loss of material is observed through rising γ_{max} and γ_{min} values upon cycling. The major role of the dimerization of native SP-B is thought to be this bridging function. The results obtained in this study strongly support this theory.

Recently, the requirement of SP-B dimerization for optimal activity was demonstrated in a mouse animal model (Beck et al., 2000). These mice expressed a monomeric SP-B mutant in an SP-B −/− background. Large aggregate surfactant from bronchoalveolar lavage and purified SP-B monomer or dimer, reconstituted with lipids, was tested and revealed slower adsorption kinetics and higher γ_{min} values during cycling experiments. Although we did not find improved adsorption for dSP-$B_{1–25}$ compared to SP-$B_{1–25}$, these results strongly support our findings.

Contrary to the results presented here, the monomeric SP-$B_{1–25}$ has been shown in monolayer studies to be able to create a reservoir of squeezed-out lipids that can reenter upon expansion (Lipp et al., 1997, 1998). This discrepancy is probably due to the dynamic system that was used in the current experiments. The differences observed for the protein-free sample with former captive bubble studies (Putz et al., 1999; Veldhuizen et al., 1999) in which the protein-free sample also creates low γ_{min} values during the whole cycling procedure are probably due to the lower lipid subphase concentration in our current experiments. Similar rising γ_{min} values are observed when no lipid vesicles are injected into the subphase (unpublished results).

A dramatic effect of PA on the peptides' activity was observed (Fig. 4 and 5). In contrast to the results with DPPC:POPG vesicles, near-zero surface tensions upon the first cycle were observed when PA was included in the

vesicles. In other words, PA somehow enhances the creation of a DPPC-enriched monolayer upon compression. We propose that the presence of PA induces a specific squeeze-out of non-DPPC lipids during compression. DPPC-poor domains within the monolayer could be more easily formed, which are then squeezed out upon compression of the bubble, leading to an almost pure DPPC monolayer at the interface. Following this theory, the adsorbed films from DPPC:POPG vesicles would contain enough DPPC to reach very low surface tensions, but fail to do so because DPPC is squeezed out together with POPG when the bubble is compressed. Interestingly, the advantageous effect of PA was not observed when hSP-B was used in adsorbed films (results not shown). The effect could therefore be specific to the combination with the peptides, or the advantageous effect of PA could be more subtle with hSP-B and only show up at lower concentrations of SP-B or in a different experimental setup.

The surface tension-area isotherms show that upon cycling increasingly less surface area reduction is needed to reach a very low surface tension (Fig. 7). This reflects an enrichment in DPPC of the monolayer. The area reduction required to reach very low surface tensions decreased significantly for both peptides upon cycling. A pure DPPC monolayer requires 15% area reduction to reach this value from equilibrium surface tension (Schürch et al., 1989, 1992), which is close to the value obtained for the SP-B_{1-25} and dSP-B_{1-25} films after a few cycles. The hSP-B sample showed a smaller effect in these decreasing values but started already with a relatively small required area reduction upon the first cycle. This implies that the monolayer was already enriched in DPPC during the initial adsorption period. This has been observed before, using the natural surfactant BLES (Schürch et al., 1992). In these experiments a fast adsorption of the material was always accompanied by lower area reductions needed to reach near-zero surface tensions. In other words, a fast adsorption results in a specific DPPC enrichment of the monolayer. The adsorption of SP-B_{1-25} and dSP-B_{1-25} in our experiments was slow (and that of hSP-B fast), and following this line of thought, no specific DPPC adsorption has occurred. This indicates that, with the synthetic peptides, the surface film is mostly enriched in DPPC because of selective squeeze-out of the non-DPPC lipids.

In summary, two peptides based on the N-terminal segment of SP-B have been tested. Both peptides contain many characteristics of the native protein in lipid mixing and captive bubble surfactometer experiments. The dimeric peptide has a clearly increased activity compared to the monomeric peptide in reservoir formation upon cycling. We presume that dimerization is required to create a lipid reservoir in close contact with the lipid monolayer at the interface and that dimerization of native SP-B has a similar function.

We gratefully acknowledge the assistance of Kym Faull of the UCLA Center for Molecular and Medical Sciences Mass Spectrometry for determination of peptide molecular mass by electrospray MS.

This research was supported by the Netherlands Foundation for Chemical Research (S.O.N.). FJW and AJW were supported by National Institutes of Health (grant HLB R01 HL55534).

REFERENCES

Andersson, M., T. Curstedt, H. Jörnvall, and J. Johansson. 1995. An amphipathic helical motif common to tumourolytic polypeptide NK-lysin and pulmonary surfactant polypeptide SP-B. *FEBS Lett.* 362: 328–332.

Baatz, J. E., B. Elledge, and J. A. Whitsett. 1990. Surfactant protein SP-B induces ordering at the surface of model membrane bilayers. *Biochemistry.* 29:6714–6720.

Beck, D. C., M. Ikegami, C. L. Na, S. Zaltash, J. Johansson, J. A. Whitsett, and T. E. Weaver. 2000. The role of homodimers in surfactant protein B function in vivo. *J. Biol. Chem.* 275:3365–3370.

Bruni, R., J. M. Hernandez-Juviel, R. Tanoviceanu, and F. J. Walther. 1998. Synthetic mimics of surfactant proteins B and C: in vitro surface activity and effects on lung compliance in two animal models of surfactant deficiency. *Mol. Gen. Metab.* 63:116–125.

Bruni, R., H. W. Taeusch, and A. J. Waring. 1991. Surfactant protein B: lipid interactions of synthetic peptides representing the amino-terminal amphipathic domain. *Proc. Natl. Acad. Sci. USA.* 88:7451–7455.

Byrne, K., J. L. Tatum, D. A. Henry, J. I. Hirsch, M. Crossland, T. Barnes, J. A. Thompson, J. Young, and H. J. Sugerman. 1992. Increased morbidity with increased pulmonary albumin flux in sepsis-related adult respiratory distress syndrome. *Crit. Care Med.* 20:28–34.

Fields, C. G., D. H. Lloyd, R. L. Macdonald, K. M. Otteson, and R. L. Noble. 1991. HBTU activation for automated Fmoc solid-phase peptide synthesis. *Pept. Res.* 4:95–101.

Gordon, L. M., S. Horvath, M. L. Longo, J. A. Zasadzinski, H. W. Taeusch, K. Faull, C. Leung, and A. J. Waring. 1996. Conformation and molecular topography of the N-terminal segment of surfactant protein B in structure-promoting environments. *Protein Sci.* 5:1662–1675.

Gordon, L. M., K. Y. C. Lee, M. M. Lipp, J. A. Zasadzinski, F. J. Walther, M. A. Sherman, and A. J. Waring. 2000. Conformational mapping of the N-terminal segment of surfactant protein B in lipid using ^{13}C-enhanced Fourier transform infrared spectroscopy. *J. Pept. Res.* 55:330–347.

Hallman, M., P. Maasilta, I. Sipila, and J. Tahvanainen. 1989. Composition and function of pulmonary surfactant in adult respiratory distress syndrome. *Eur. Respir. J. Suppl.* 3:104s–108s.

Johansson, J., G. Nilsson, R. Stromberg, B. Robertson, H. Jörnvall, and T. Curstedt. 1995. Secondary structure and biophysical activity of synthetic analogues of the pulmonary surfactant polypeptide SP-C. *Biochem. J.* 307:535–541.

Johansson, J., T. Szyperski, T. Curstedt, and K. Wuthrich. 1994. The NMR structure of the pulmonary surfactant-associated polypeptide SP-C in an apolar solvent contains a valyl-rich alpha-helix. *Biochemistry.* 33: 6015–6023.

Jorens, P. G., J. van Damme, W. de Backer, L. Bossaert, R. F. de Jongh, A. G. Herman, and M. Rampart. 1992. Interleukin 8 (IL-8) in the bronchoalveolar lavage fluid from patients with the adult respiratory distress syndrome (ARDS) and patients at risk for ARDS. *Cytokine.* 4:592–597.

Lipp, M. M., K. Y. C. Lee, D. Y. Takamoto, J. A. Zasadzinski, and J. A. Waring. 1998. Coexistence of buckled and flat monolayers. *Phys. Rev. Lett.* 81:1650–1653.

Lipp, M. M., K. Y. C. Lee, A. J. Waring, and J. A. Zasadzinski. 1997. Fluorescence, polarized fluorescence, and Brewster angle microscopy of palmitic acid and lung surfactant protein B monolayers. *Biophys. J.* 72:2783–2804.

Lipp, M. M., K. Y. C. Lee, J. A. Zasadzinski, and A. J. Waring. 1996. Phase and morphology changes in lipid monolayers induced by SP-B protein and its amino-terminal peptide. *Science.* 273:1196–1199.

Longo, M. L., A. M. Bisagno, J. A. Zasadzinski, R. Bruni, and A. J. Waring. 1993. A function of lung surfactant protein SP-B. *Science.* 261:453–456.

Matsumoto, K., F. Taki, Y. Kondoh, H. Taniguchi, and K. Takagi. 1992. Platelet-activating factor in bronchoalveolar lavage fluid of patients with adult respiratory distress syndrome. *Clin. Exp. Pharmacol. Physiol.* 19:509–515.

Nakos, G., J. Pneumatikos, I. Tsangaris, C. Tellis, and M. Lekka. 1997. Proteins and phospholipids in BAL from patients with hydrostatic pulmonary edema. *Am. J Respir. Crit. Care Med.* 155:945–951.

Nilsson, G., M. Gustafsson, G. Vandenbussche, E. J. A. Veldhuizen, W. J. Griffiths, J. Sjovall, H. P. Haagsman, J. M. Ruysschaert, B. Robertson, T. Curstedt, and J. Johansson. 1998. Synthetic peptide-containing surfactants—evaluation of transmembrane versus amphipathic helices and surfactant protein C poly-valyl to poly-leucyl substitution. *Eur. J. Biochem.* 255:116–124.

Nogee, L. M., G. Garnier, H. C. Dietz, L. Singer, A. M. Murphy, D. E. deMello, and H. R. Colten. 1994. A mutation in the surfactant protein B gene responsible for fatal neonatal respiratory disease in multiple kindreds. *J. Clin. Invest.* 93:1860–1863.

Oosterlaken-Dijksterhuis, M. A., H. P. Haagsman, L. M. G. van Golde, and R. A. Demel. 1991. Characterization of lipid insertion into monomolecular layers mediated by lung surfactant proteins SP-B and SP-C. *Biochemistry.* 30:10965–10971.

Oosterlaken-Dijksterhuis, M. A., M. van Eijk, L. M. G. van Golde, and H. P. Haagsman. 1992. Lipid mixing is mediated by the hydrophobic surfactant protein SP-B but not by SP-C. *Biochim. Biophys. Acta.* 1110:45–50.

Patthy, L. 1991. Homology of the precursor of pulmonary surfactant-associated protein SP-B with prosaposin and sulfated glycoprotein 1. *J. Biol. Chem.* 266:6035–6037.

Perez-Gil, J., and K. M. W. Keough. 1998. Interfacial properties of surfactant proteins. *Biochim. Biophys. Acta.* 1408:203–217.

Putz, G., J. Goerke, S. Schürch, and J. A. Clements. 1994. Evaluation of pressure-driven captive bubble surfactometer. *J. Appl. Physiol.* 76: 1417–1424.

Putz, G., M. Walch, M. van Eijk, and H. P. Haagsman. 1998. A spreading technique for forming film in a captive bubble. *Biophys. J.* 75: 2229–2239.

Putz, G., M. Walch, M. van Eijk, and H. P. Haagsman. 1999. Hydrophobic lung surfactant proteins B and C remain associated with surface film during dynamic cyclic area changes. *Biochim. Biophys. Acta.* 1453: 126–134.

Robertson, B., and H. L. Halliday. 1998. Principles of surfactant replacement. *Biochim. Biophys. Acta.* 1408:346–361.

Schürch, S., H. Bachofen, J. Goerke, and F. Possmayer. 1989. A captive bubble method reproduces the in situ behavior of lung surfactant monolayers. *J. Appl. Physiol.* 67:2389–2396.

Schürch, S., F. Possmayer, S. Cheng, and A. M. Cockshutt. 1992. Pulmonary SP-A enhances adsorption and appears to induce surface sorting of lipid extract surfactant. *Am. J. Physiol.* 263:L210–L218.

Schürch, S., R. Qanbar, H. Bachofen, and F. Possmayer. 1995. The surface-associated surfactant reservoir in the alveolar lining. *Biol. Neonate.* 67(Suppl. 1):61–76.

Takei, T., Y. Hashimoto, T. Aiba, K. Sakai, and T. Fujiwara. 1996. The surface properties of chemically synthesized peptides analogous to human pulmonary surfactant protein SP-C. *Biol. Pharm. Bull.* 19: 1247–1253.

Tokieda, K., J. A. Whitsett, J. C. Clark, T. E. Weaver, K. Ikeda, K. B. McConnell, A. H. Jobe, M. Ikegami, and H. S. Iwamoto. 1997. Pulmonary dysfunction in neonatal SP-B-deficient mice. *Am. J. Physiol.* 273: L875–L882.

Veldhuizen, E. J. A., J. J. Batenburg, G. Vandenbussche, G. Putz, L. M. G. van Golde, and H. P. Haagsman. 1999. Production of surfactant protein C in the baculovirus expression system: the information required for correct folding and palmitoylation of SP-C is contained within the mature sequence. *Biochim. Biophys. Acta.* 1416:295–308.

Waring, A. J., W. Taeusch, R. Bruni, J. Amirkhanian, B. Fan, R. Stevens, and J. Young. 1989. Synthetic amphipathic sequences of surfactant protein-B mimic several physicochemical and in vivo properties of native pulmonary surfactant proteins. *Pept. Res.* 2:308–313.